Journal of Cerebral Blood Flow & Metabolism (2015) 35, 1977–1984

www.jcbfm.com

ORIGINAL ARTICLE

MicroRNA-29b is a therapeutic target in cerebral ischemia associated with aquaporin 4

Yang Wang[1,4], Jun Huang[2], Yuanyuan Ma[1], Guanghui Tang[2], Yanqun Liu[1], Xiaoyan Chen[2], Zhijun Zhang[2], Lili Zeng[1], Yongting Wang[2], Yi-Bing Ouyang[3] and Guo-Yuan Yang[1,2]

MicroRNA-29b (miR-29b) is involved in regulating ischemia process, but the molecular mechanism is unclear. In this work, we explored the function of miR-29b in cerebral ischemia. The level of miR-29b in white blood cells was evaluated in patients and mice after ischemic stroke. Brain infarct volume and National Institute of Health stroke scale (NIHSS) scores were analyzed to determine the relationship between miR-29b expression and the severity of stroke. The relationship of miR-29b and aquaporin-4 (AQP4) was further studied in mice. We found that miR-29b was significantly downregulated in stroke patients ($P < 0.05$). MiR-29b level negatively associated with NIHSS scores ($r = -0.349$, $P < 0.01$) and brain infarct volume ($r = -0.321$, $P < 0.05$). In ischemic mice, miR-29b in the brain and blood were both downregulated ($r = 0.723$, $P < 0.05$). MiR-29b overexpression reduced infarct volume (49.50 ± 6.55 versus $35.48 \pm 2.28\ mm^3$, $P < 0.05$), edema ($164 \pm 4\%$ versus $108 \pm 4\%$, $P < 0.05$), and blood–brain barrier (BBB) disruption compared with controls ($15 \pm 9\%$ versus $7 \pm 3\%$, $P < 0.05$). Aquaporin-4 expression greatly decreased after miR-29b overexpression ($28 \pm 7\%$ versus $11 \pm 3\%$, $P < 0.05$). Dual-luciferase reporter system showed that AQP-4 was the direct target of miR-29b ($P < 0.05$). We concluded that miR-29b could potentially predict stroke outcomes as a novel circulating biomarker, and miR-29b overexpression reduced BBB disruption after ischemic stroke via downregulating AQP-4.

Journal of Cerebral Blood Flow & Metabolism (2015) **35,** 1977–1984; doi:10.1038/jcbfm.2015.156; published online 1 July 2015

Keywords: aquaporin-4; human; ischemia; microRNA-29b; stroke

INTRODUCTION

Acute ischemic stroke often results in the breakdown of blood–brain barrier (BBB) and leads to vasogenic edema.[1] Aquaporin-4 (AQP4) is an important water-channel protein in the central nervous system (CNS).[2] It is particularly expressed at the perivascular foot processes of astrocytes, glia membranes, and ependymal cells.[3,4] Cerebral ischemia upregulates AQP4 expression, increases BBB permeability, and induces brain edema, which exacerbates ischemic brain injury. The level of AQP4 messenger RNA (mRNA) increases and peaks on day 3 after middle cerebral artery occlusion (MCAO) in rats.[5] Aquaporin-4 knockout in mice protects neurocytes against cytotoxic edema caused by water intoxication and permanent focal cerebral ischemia.[6] It was reported recently that mesenchymal stem cells maintained BBB integrity by inhibiting AQP4 upregulation after cerebral ischemia.[7] However, the underlying molecular mechanism, especially at transcriptional or post-transcriptional levels, of AQP4 upregulation is unknown.

Recent studies have highlighted the potential regulation of microRNA (miRNA) for the downstream target gene in cerebral ischemia.[8] MicroRNAs are single-stranded noncoding RNA molecules of ~22 nucleotides in length, which function as regulators of gene expression by binding to the 3′ untranslated region (UTR) of mRNA molecules and destabilizing them or inhibiting their translation.[9] MiR-29 family members, including miR-29a, 29b, and 29c, are highly conserved in human and rodents.[10] After transient MCAO, 11 miRNAs including miR-29b showed altered expression at 4 of the 5 time points evaluated (3 hours to 3 days reperfusion), among which miR-29b exhibited the most significant downregulation at day 1 and day 3 after ischemia/reperfusion.[11] Earlier study implicated that miR-29b was markedly induced during neuronal maturation and functioned as a novel inhibitor of neuronal apoptosis through targeting BH3-only genes.[12] The level of miR-29b decreased after acute ischemic stroke, contributing to neural cell death and brain infarction.[13]

With the help of bioinformatic-based databases[14] and published reports,[15,16] we found that AQP4 might be a potential direct target of miR-29b. The present study validated for the first time that indeed miR-29b regulated AQP4 level. We explored the level of miR-29b in acute ischemic stroke patients and in mice with MCAO surgery as well as the relationship among miR-29b, AQP4, and BBB integrity. We concluded that miR-29b could potentially predict stroke outcomes as a novel circulating biomarker, and that miRNA-29b overexpression protected the integrity of the BBB after ischemic stroke by potentially downregulating AQP-4.

[1]Department of Neurology, Ruijin Hospital, Shanghai Jiao Tong University, School of Medicine, Shanghai, China; [2]Neuroscience and Neuroengineering Research Center, Med-X Research Institute and School of Biomedical Engineering, Shanghai Jiao Tong University, Shanghai, China and [3]Department of Anesthesia, Stanford University School of Medicine, Stanford, California, USA. Correspondence: Dr G-Y Yang, Neuroscience and Neuroengineering Research Center, Med-X Research Institute and School of Biomedical Engineering, Shanghai Jiao Tong University, 1954 Hua Shan Road, Shanghai 200030, China.
E-mail: gyyang0626@163.com
[4]Current address: Department of Neurology, Central Hospital of Wuhan, Wuhan 430000, China.
The study is supported by the National Key Basic Research Program of China, 973 Program, 2011CB504405 (G-YY, YW), the National Natural Science Foundation of China, U1232205 (G-YY) and 81371305 (YW), Shanghai Jiao Tong University Foundation for technological innovation of major projects 12X190030021 (G-YY) and KC Wong Foundation (G-YY), Science and Technology Commission of Shanghai Municipality, 13ZR1422600 (ZZ).
Received 15 January 2015; revised 14 May 2015; accepted 15 May 2015; published online 1 July 2015

MATERIALS AND METHODS

Clinical Patient Selection

Human project was approved by the committee of Institutional Review Board of Shanghai Jiao Tong University, Shanghai, China. Written informed consent was obtained from patients according to the Helsinki Declaration and the Helsinki Declaration was followed during the human studies. The control group was recruited from subjects who matched age and sex to the stroke patients. Acute ischemic stroke was diagnosed by neurologists according to physical examination and radiologic diagnosis. The exclusion criteria included recurrent stroke, intracranial tumor, multiple trauma, hematological system diseases, renal or liver failure, acute infection, and other diseases affecting the hemogram. Finally, demographic changes, associated laboratory inspection, and imaging information, which included blood pressure, fasting blood glucose, cholesterol, triglyceride, computed tomography, magnetic resonance imaging, magnetic resonance angiography, carotid artery ultrasonography, and cardiac ultrasonography, were also collected to determine the relationship between the changes of miR-29 and the characteristics of clinical parameters.

National Institute of Health stroke scale (NIHSS) scores and the modified Rankin score were performed by clinical neurologists to assess the severity and prognosis of ischemic stroke at 3 month after the stroke onset.[17] Modified Rankin score < 2 was defined as a good outcome and modified Rankin score $\geqslant 2$ was defined as a poor outcome.[18] Risk factors included: hypertension: blood pressure above 140/90 mm Hg; hyperlipidemia: total cholesterol level $\geqslant 6.7$ mmol/L, triglyceride level $\geqslant 1.8$ mmol/L and high-density lipoprotein level $\leqslant 1$ mmol/L; diabetes mellitus: fasting-blood glucose level > 6.1 mmol/L or HbA1c $\geqslant 7\%$. The infarct volume was calculated by ABC/2 method.[19]

Stroke Patients Blood Preparation and RNA Extraction

The blood sample was collected within 72 hours after stroke symptom onset. A human blood sample (4 mL) was collected into tubes containing ethylenediaminetetraacetic acid (EDTA), and centrifuged at 1,500 *g* for 10 minutes at 4°C immediately. Then, the erythrocytes were dissociated with erythrocyte lysing solution and discarded, the remaining white blood cells were saved for the total RNA extraction. Total RNA was extracted using TRIzol method according to the manufacturer's instructions (Invitrogen, Carlsbad, CA, USA). The integrity and concentration of total RNA was quantified using a NanoDrop 1000 spectrophotometer (Thermo, Wilmington, DE, USA).

Animal Experiment Design

Animal studies were reported in accordance with ARRIVE guidelines. Procedure for the use of laboratory animals was approved by the Institutional Animal Care and Use Committee of Shanghai Jiao Tong University, Shanghai, China. During the animal studies, guidelines of *the regulation for the administration of affairs concerning experimental animals of China* enacted in 1988 were followed. Mice were housed in home cage under standard laboratory conditions. Adult male CD-1 mice ($n = 54$) weighing 25 to 30 g were divided into three groups: Lentivirus-miR-29b (LV-29b)-treated ($n = 18$), LV-GFP-treated ($n = 18$), and normal saline (NS)-control groups ($n = 18$). Middle cerebral artery occlusion (MCAO) surgery was performed at 14 days after viral vector transduction or NS injection. Mice were killed at 1 day and 3 days after MCAO. MiR-29b levels in the brain and blood of mice were detected by reverse transcription and real-time PCR. Brain infarct volume was measured by cresyl violet staining. The integrity of BBB and the expression of AQP4 were further evaluated by immune-staining and western blot.

Animal Brain Sample Preparation

The mouse brain was rapidly removed after killing animals and cut into four coronal sections with 2 mm thickness. The second slice was divided into ipsilateral and contralateral halves. The total RNA in ipsilateral brain tissue was extracted using TRIzol LS method (Invitrogen) according to the manufacturer's instructions. RNA concentration and purity were detected by a NanoDrop 1000 spectrophotometer (Thermo).

Reverse Transcription and Real-Time PCR

First-strand cDNA was synthesized from 10 ng total RNA using EXIQON universal cDNA synthesis kit (EXIQON, Vedbaek, Denmark). The amplification was performed by a fast real-time PCR system (7900 HT, ABI, Foster City, CA, USA) using SYBR Green master mix and Universal RT kit (EXQION, Woburn, MA, USA). A 384-well plate was run following the cycling condition: 95°C for 10 minutes followed by 40 cycles of 95°C for 10 seconds and 60°C for 1 minute. The relative expression level of miR-29b was normalized to the endogenous control U6 in triplicate and was calculated by the $2^{-\Delta ct}$ method.[20]

Lentivirus-miR-29b Production

Lentivirus was packaged and tittered as described previously.[21] Briefly, pGIPZ-miR-29b, VSVG plasmid, and *p* delta plasmid were cotransfected into 293 T cells. Twenty-four hours after transfection, cells were switched to virus production medium (Ultraculture+Penicillin/ streptomycin+Sodium Pyruvate+Sodium Butyrate). The supernatant was collected at 48 and 72 hours after transfection and the virus was purified with sucrose density gradient centrifugation.[22] The viral titer was determined by FACS analysis after purification. Lentivirus-green fluorescent protein, as a viral marker and a viral control, was prepared with the same protocol.

Lentivirus-miR-29b Gene Transfer into the Mouse Brain

Adult male CD-1 mice were anesthetized with ketamine/xylazine (100 mg/10 mg/kg, Sigma, St. Louis, MO, USA). Mice were then fixed on a stereotactic frame (RWD, Shenzhen, China). Each mice received a dose of LV-29b (3.0×10^6 IU in 3 μL NS), LV-GFP or 3 μL NS vehicle control. The liquid was slowly injected into the left striatum (AP = − 0.02 mm, ML = − 2.5 mm, DV = 3) at a rate of 0.2 μL/min via a mini-pump (WPI, Sarasota, FL, USA) as described previously.[23] At 14 days after viral vector injection, MCAO model was performed on these mice.

Middle Cerebral Artery Occlusion in Mice

The procedure of MCAO was described in our previous study.[24] Mice were anesthetized with ketamine/xylazine. Body temperature was maintained at 37 ± 0.3°C using a heating pad (RWD Life Science) during the anesthesia. Left common carotid artery, external carotid artery and internal carotid artery were carefully isolated. A small cut was made on the external carotid artery and a 2.0 cm silicone-coated 6-0 nylon suture (Covidien, Mansfield, MA, USA) was gently inserted from the external carotid artery stump to the internal carotid artery, and stopped at the opening of MCA. The distance from the bifurcation of internal carotid artery/external carotid artery to middle cerebral artery was 10 ± 0.5 mm. Successful occlusion was verified by a laser Doppler flowmeter (Moor Instruments, Devon, UK). We measured the mouse cortical blood flow before MCAO as a baseline blood flow. Mice were excluded if the cortical blood flow was greater than 15% of the baseline. Sham-operated mice underwent the same surgery procedure without insertion of the suture into the internal carotid artery.

Determination of Brain Infarct Volume and Edema Formation

The brain infarct and the edema volume were measured as described in the previous study.[25] Brains were rapidly removed and frozen immediately after killing animals at 1 day and 3 days after MCAO. Brain infarct and edema volume were measured using cresyl violet staining. A series of 20 μm frozen coronal sections from anterior commissure to hippocampus were cut. The distance between sections is 200 μm. A total of 20 sections were counted. The infarct area of each section was delineated blindly and infarct volume was calculated using the following formula: $V = \sum_1^n \left[(S_n + \sqrt{S_n * S_{n+1}} + S_{n+1}) * \frac{h}{3} \right]$, in which h was the distance between two sections. Brain edema formation was calculated as (1 − (total ipsilateral hemisphere − infarct)/total contralateral hemisphere) × 100%. Image analysis software (NIH Image J, Bethesda, MD, USA) was used for infarct volume determination.

Blood–Brain Barrier Function Was Examined by Immune-Staining and Western Blot

IgG immunostaining was performed as reported.[26] Briefly, brain slices were incubated with biotinylated universal antibody (Vector Laboratories, Burlingame, CA, USA) for 1 hour, then incubated with Vectastain ABC reagent for 1 hour. The reaction product was visualized using DAB staining. Images were analyzed by Image Pro Plus 6.0 (Media Cybernetic, Bethesda, MD, USA).

For zonula occludens-1 (ZO-1) and occludin immunofluorescent staining, brain sections were fixed with 4% paraformaldehyde for 10 minutes and incubated in phosphate-buffered saline containing 0.1%

Triton X-100 for 10 minutes. Then, 10% BSA blocked for 1 hour and incubated with anti-ZO-1 or anti-Occludin (1:100 dilution, Invitrogen) antibodies overnight at 4°C. Brain sections were then incubated with fluorescence-conjugated secondary antibodies. Images were photographed by a confocal microscope (Leica, Solms, Germany). The vessels we interested in our study were microvessels between 4 and15 μm since BBB leakage occurred at that level. In normal microvessels, ZO-1 and occludin were continuously and clearly presented on the endothelial cell margin ($CD31^+$). The relative gap length of microvessels was quantified from three fields per section of five serial sections, which were 200 μm apart in each animal, which was presented as percentages of whole tight junction protein staining.[27]

The mouse brain tissue was collected and the protein concentrations were determined with a BCA kit (Thermo Scientific, Waltham, UK). Proteins (40 μg) were loaded onto 10% resolving gel for eclectrophoresis. Proteins were transferred onto a nitrocellose membrane (Whatman Inc., Florham Park, NJ, USA) and blocked with 5% skim milk. Then, the membrane was incubated with primary anti-AQP4 (1:500 dilution, Santa Cruz Biotechnology, Dallas, TX, USA) and anti-β-actin (1:1,000 dilution, Sigma, St. Louis, MO, USA) antibodies overnight at 4°C, respectively. Membranes were incubated with horseradish peroxidase-conjugated secondary antibodies and then reacted with an enhanced chemiluminescenece substrate (Prierce, Rockford, IL, USA). The results of chemiluminescence were recorded with an imaging system (Bio-Rad, Hercules, CA, USA).

Dual Luciferase Reporter Assay

Each fragment of the 3′UTR and mutant 3′UTR of AQP4 was amplified and cloned into a pGL3 vector containing the firefly luciferase reporter gene (Promega, Madison, WI, USA). For the luciferase reporter assay, 293 T cells were cotransfected with 200 ng firefly luciferase constructs, 4 ng pRL-TK renilla luciferase plasmid, and 50 nmol/L synthetic miR-29b mimic molecules. Renilla luciferase activity was measured using a dual-luciferase reporter assay (Promega) 48 hours after transfection. The results were expressed as relative luciferase activity (firefly luciferase/renilla luciferase).

Statistical Analysis

The results were expressed as percentages for categorical variables and as mean ± s.d. or median and range (25th and 75th percentiles) for the continuous variables depending on whether their distribution was normal or not. The Kolmogorov–Smirnov test was used for testing the normality of the distribution. Proportions were compared using a Chi-square test, while the continuous variables between groups were compared with the Student's *t* or Mann–Whitney test. Spearman's analysis was used for bivariate correlations depending on their non-normal distribution. ANOVA was used for comparison among several quantitative variables. The influence of miR-29b level on a categorical variable was assessed by logistic regression analysis using forward stepwise selection procedures after adjusting for those variables with a proven biological relevance for stoke morbidity to avoid the possibility of finding some spurious associations. Results were expressed as adjusted odds ratios with the corresponding 95% confidence intervals. Statistical analysis was determined using SPSS 18.0 software (SPSS, Chicago, IL, USA) and a probability $P < 0.05$ was considered as statistical significance.

RESULTS

The Characteristics of Patients

The characteristics of ischemic stroke patients ($n = 58$) and controls ($n = 59$) enrolled in this study were shown in Supplementary Table 1. Stroke patients (mean age: 62, male/female = 44/14) had no difference to the control group either in age ($P = 0.225$) or in sex ($P = 0.44$). Stroke patients had higher risks than the controls. To eliminate the unmatched factors (hypertension, diabetes, and hyperlipidemia) impaction on miR-29b expression between two groups, we performed a logistic regression. The result indicated that miR-29b level was variable for the stroke occurrence ($P = 0.039$).

Circulating miR-29b Expression Level Decreased in Stroke Patients

We first showed that miR-29b expression level decreased in stroke group compared with control group (Figure 1A, $P < 0.05$). To assess the potential role of miR-29b in stroke pathogenesis, we examined the relationship between miR-29b expression level and NIHSS scores and brain infarct volume. We found that miR-29b level was higher in patients with good outcomes compared to

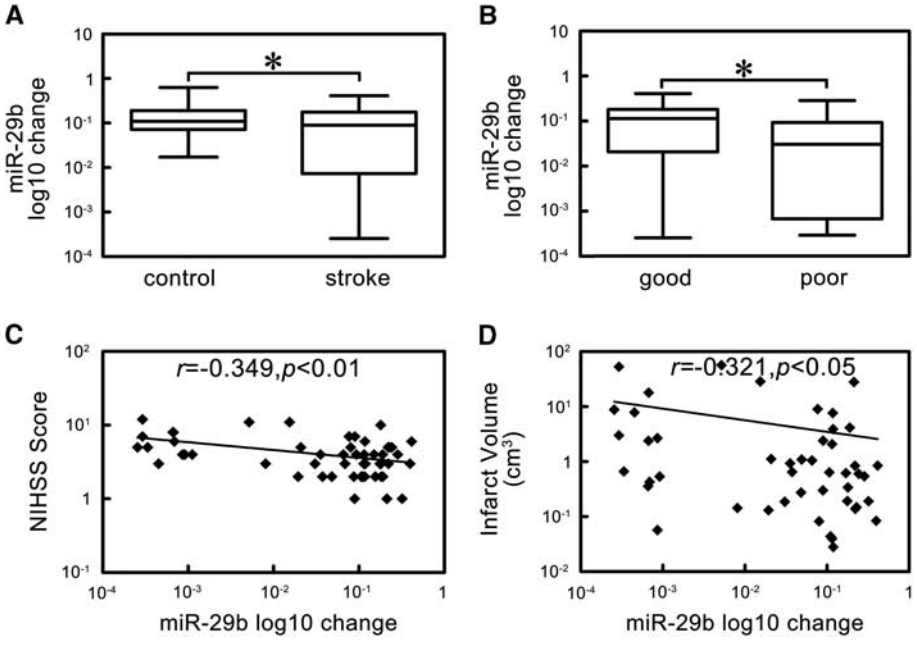

Figure 1. The expression and correlation analysis of microRNA-29b (miR-29b) in ischemic stroke patients. (**A**) Box plot of miR-29b expression levels in stroke patients and control. *$P < 0.05$, stroke versus control, $n = 58$ in stroke group, $n = 59$ in control group. (**B**) Box plot of miR-29b expression levels in patients with good and poor outcomes. *$P < 0.05$, good group versus poor group, $n = 43$ in good group, $n = 15$ in poor group. (**C**) Scatter plot of the relationship between miR-29b and National Institute of Health stroke scale (NIHSS) scores. $r = -0.349$, $P < 0.01$. (**D**) Scatter plot of the relationship between miR-29b and infarct volume. $r = -0.321$, $P < 0.05$. miR-29b expression level is changed by log10.

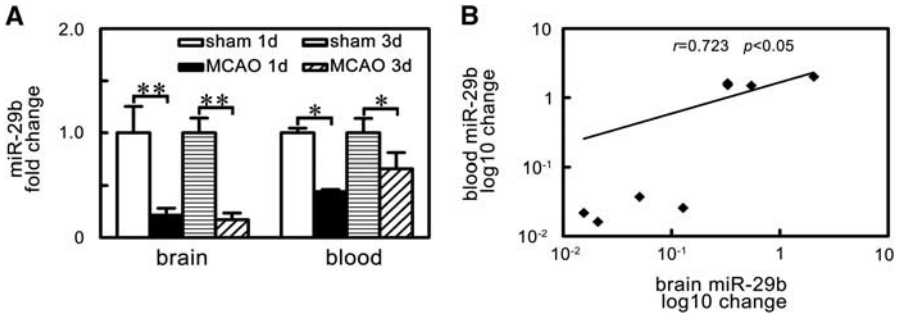

Figure 2. MicroRNA-29b (miR-29b) levels paralleled decreased in brain tissue and blood of ischemic mice. (**A**) Bar graph of the expression levels of miR-29b in brain tissue and blood of sham group and middle cerebral artery occlusion (MCAO) group at 1 day and 3 days after ischemia. *$P < 0.05$; **$P < 0.01$, MCAO versus sham. $n = 4$/group. (**B**) Scatter plot showed the correlation between brain miR-29b expression and blood miR-29b expression. $r = 0.723$, $P < 0.05$. miR-29b expression levels are changed by log10.

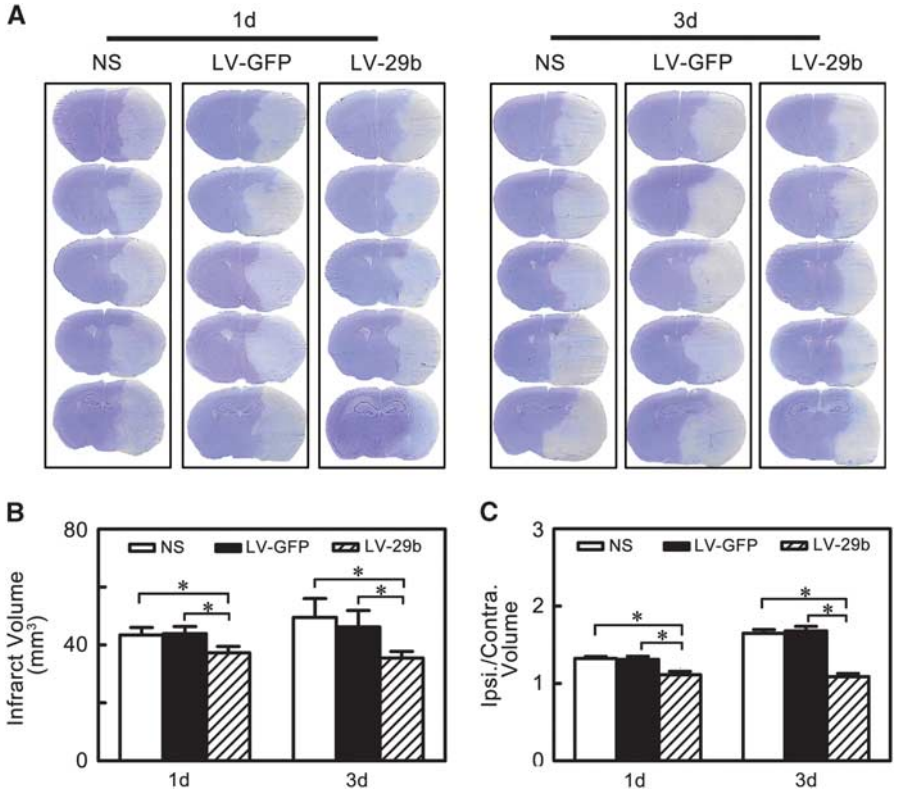

Figure 3. MicroRNA-29b (miR-29b) overexpression reduced brain infarction and edema at 1 day and 3 days after middle cerebral artery occlusion (MCAO). (**A**) A series of coronal sections represented brain infarction in normal saline (NS), LV-GFP-, and LV-miR-29b-injected groups of mice. (**B**) Bar graph of calculated infarct volume. *$P < 0.05$, data are mean ± s.d., $n = 6$ per group in each time point. (**C**) Bar graph of calculated brain edema volume. *$P < 0.05$, data are mean ± s.d., $n = 6$ per group in each time point. LV, lentivirus.

those with poor outcomes (Figure 1B, $P < 0.05$). MiR-29b expression negatively associated with NIHSS scores (Figure 1C, $r = -0.349$, $P < 0.01$) and brain infarct volume (Figure 1D, $r = -0.321$, $P < 0.05$).

MicroRNA-29b Expression Paralleled in Blood and Brain Tissue After Ischemic Stroke

To determine the relationship of miR-29b expression between circulating blood and brain tissue, we examined the blood and brain tissue miR-29b in the same animal. We found that the decreased miR-29b expression in the brain tissue paralleled with that in the circulating blood after MCAO in mice (Figure 2A, $P < 0.05$). Further correlation analysis showed that brain miR-29b expression was positively correlated with circulating blood miR-29b level (Figure 2B, $r = 0.723$, $P < 0.05$).

MicroRNA-29b Overexpression Reduced Infarct Volume and Edema Formation in Middle Cerebral Artery Occlusion Mice

To increase miR-29b expression in the brain, we used LV-miR-29b gene transfer. We showed that miR-29b expression was greatly increased after LV-miR-29b injection. MiR-29b was highly expressed in the LV-miR-29b-injected hemisphere in the mouse brain (Supplementary Figure 1, $P < 0.05$), suggesting the success of LV-miR-29b gene transduction.

After the miR-29b overexpression, we further characterized the brain infarct volume to evaluate the effect of miR-29b overexpression. We found that the infarct volume significantly decreased in the LV-miR-29b-treated group at 1 day and 3 days after MCAO compared with the LV-GFP-treated and saline control groups (Figure 3B, $P < 0.05$). Similar to the infarct volume measurement, we found that the edema formation of ipsilateral hemisphere in LV-miR-29b treated mice was significantly lower than that in the control mice after MCAO (Figure 3C, $P < 0.05$).

MicroRNA-29b Overexpression Attenuated Blood–Brain Barrier Disruption in Ischemic Mice

To evaluate BBB permeability after ischemic brain injury, IgG protein extravasation was measured. Extravasated IgG significantly increased after MCAO while markedly decreased in the LV-miR-29b-treated mice compared with the controls (Figure 4A, $P < 0.01$). To investigate the mechanism of BBB disruption, we analyzed the localization of ZO-1 and occludin in cerebral vascular structures using CD31/occludin and CD31/ZO-1 double staining. Confocal microscopy analysis showed that the ZO-1 and occludin continuity was disrupted after MCAO in mice. It was noted that this pathologic change was reversed and gap formation was greatly reduced in the LV-miR-29b-treated mice after MCAO (Figure 4B and 4C, $P < 0.05$).

MicroRNA-29b Overexpression Inhibited Aquaporin 4 Upregulation After Middle Cerebral Artery Occlusion in Mice

To understand the molecular mechanism regulated by miR-29b in the ischemic stroke, we searched for possible downstream targets of miR-29b in Target Scan 6.0 (http://www.targetscan.org) and PicTar (http://pictar.org), which were the online resources for miRNAs analysis.[28] We found that miR-29b could recognize AQP4 mRNA 3′UTR (Figure 5Ca). We showed that both AQP4 mRNA and protein level after MCAO were significantly upregulated (Figure 5A: *Left and Right*, $P < 0.05$). To determine whether miR-29b inhibited AQP4 expression, we examined AQP4 mRNA and protein in the LV-miR-29b-treated mice after MCAO. We found that AQP4 protein expression was reduced in the LV-miR-29b-treated mice compared with the control mice (Figure 5B**:** *Right,* $P < 0.05$). Reduced AQP4 mRNA was observed in the LV-miR-29b treated mice at 3 days after MCAO (Figure 5B**:** *Left,* $P < 0.05$). To confirm whether AQP4 was regulated by miR-29b, we cloned AQP4 mRNA 3′UTR fragment and mutant 3′UTR fragment containing the putative miR-29b binding sites upstream of the luciferase coding sequence and performed co-transfection of the luciferase reporter and miR-29b mimic in 293 T cells (Figure 5Cb). Luciferase activity level was reduced in the cells cotransfected with miR-29b mimic and AQP4 mRNA 3′UTR fragment compared with the miR-29b mimic and the mutant 3′UTR fragment group or with AQP4 mRNA 3′UTR fragment only (Figure 5Cc, $P < 0.01$). These results suggest that AQP4 is a direct target of miR-29b.

DISCUSSION

There were two novel aspects of the current study: (1) clinically as a novel circulating biomarker, miR-29b could potentially predict stroke outcomes; (2) mechanistically as a downregulator of AQP4, miR-29b attenuated ischemia-induced BBB disruption and brain edema formation, and reduced infarction volume after cerebral ischemia.

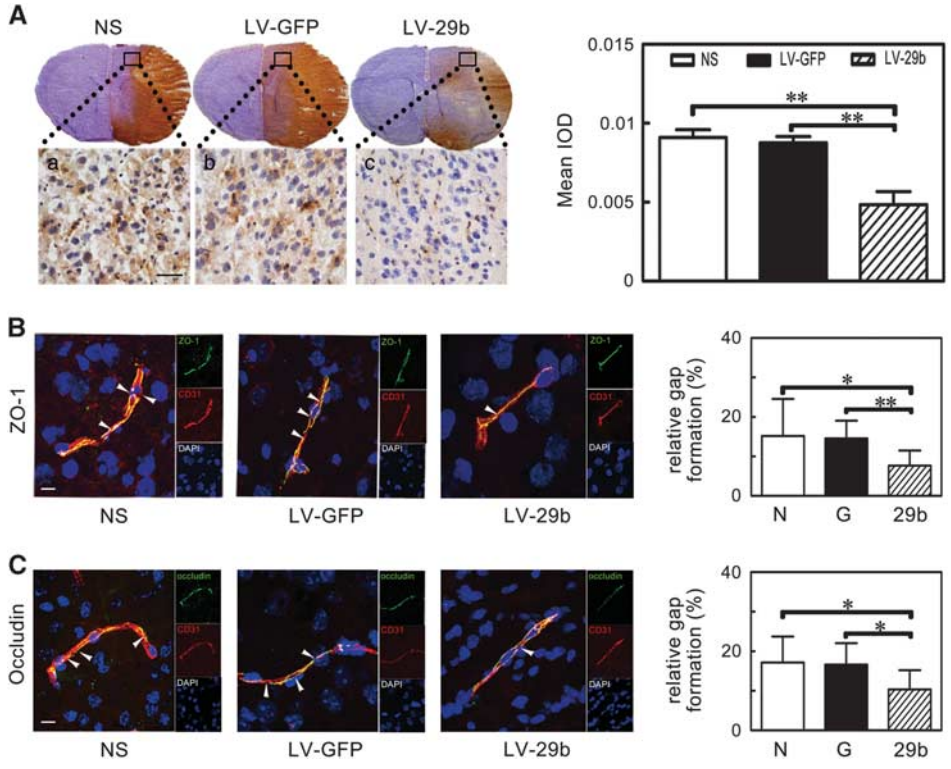

Figure 4. IgG leakage and the breakage of zonula occludens-1 (ZO-1) and occludin were attenuated after microRNA-29b (miR-29b) overexpression. (**A**) Photomicrography represented IgG staining in the ischemic perifocal region in the LV-miR-29b-, LV-GFP-, and saline-treated mice after 3 days of middle cerebral artery occlusion (MCAO). Subpanels (a–c) were magnified to the box region. Scale bar = 100 μm. Bar graph showed the quantification of IgG leakage. $^{**}P < 0.01$, data are mean ± s.d., $n = 6$ per group. (**B** and **C**) The microphotograph presented tight junction protein ZO-1 and occludin immunostaining in perifocal region after 3 days of MCAO in the LV-miR-29b-, LV-GFP-, and saline-injected groups. The arrowhead indicated the gap caused by ZO-1 and occludin protein destruction. Bar graph showed the quantification of gap length. $^{*}P < 0.05$; $^{**}P < 0.01$, data are mean ± s.d., $n = 6$ per group. G: LV-GFP; 29b: LV-miR-29b; LV, lentivirus; N: normal saline.

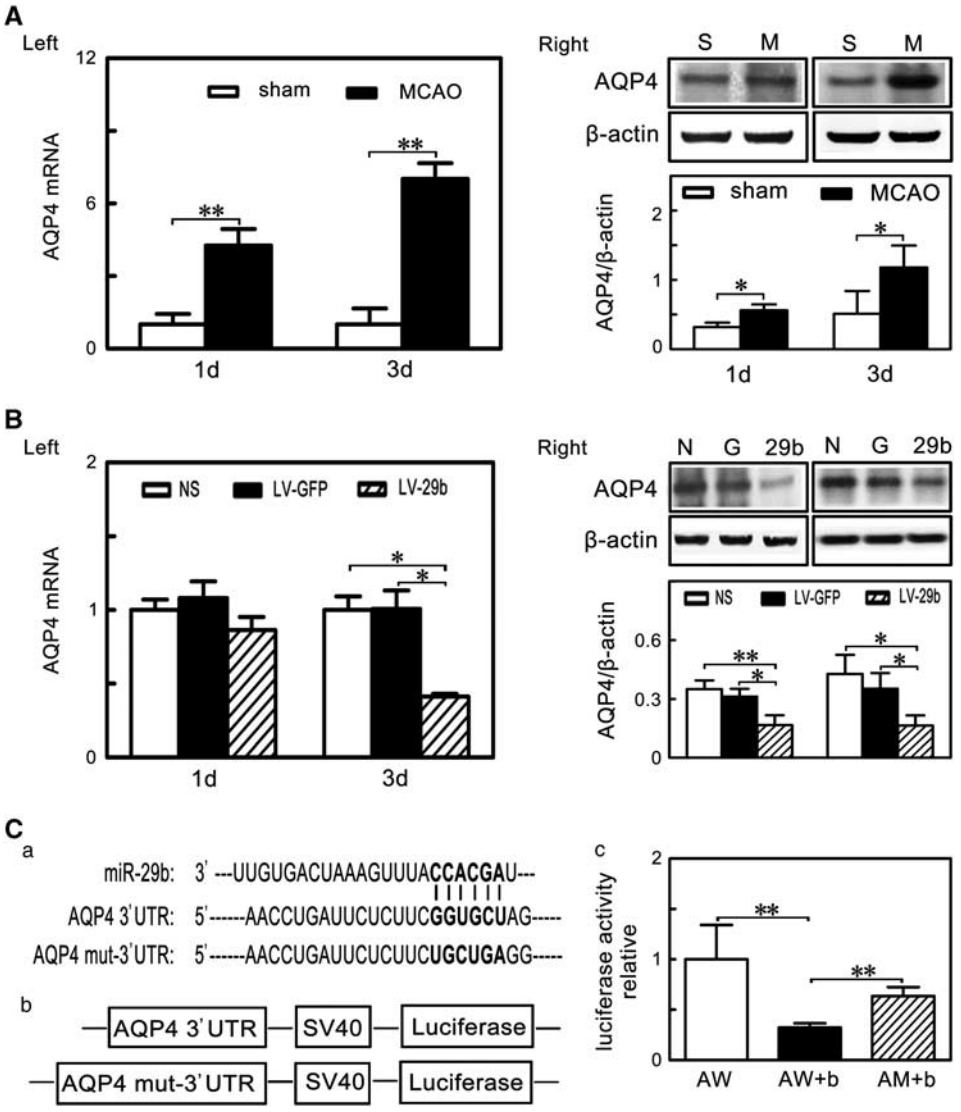

Figure 5. MicroRNA-29b (miR-29b) overexpression inhibited aquaporin 4 (AQP4) upregulation after middle cerebral artery occlusion (MCAO). (**A**) *Left*: Bar graph showed AQP4 messenger RNA (mRNA) expression in sham and MCAO group at 1 day and 3 days after MCAO. $^{**}P < 0.01$, data are mean ± s.d., $n = 3$ per group. *Right*: Western blot showed AQP4 expression in sham and MCAO group at 1 day and 3 days after MCAO. $^{*}P < 0.05$, data are mean ± s.d., $n = 3$ per group. (**B**) *Left:* Bar graph showed AQP4 mRNA expression in NS, LV-GFP and LV-miR-29b group at 1 day and 3 days after MCAO. $^{*}P < 0.05$, data are mean ± s.d., $n = 3$ per group. *Right:* Western blot showed AQP4 expression in NS, LV-GFP, and LV-miR-29b group at 1 day and 3 days after MCAO. $^{*}P < 0.05$; $^{**}P < 0.01$, data are mean ± s.d., $n = 3$ per group. (**C**) (a) Schematic representation of miR-29b recognition site in AQP4 3′ untranslated region (UTR) and AQP4 mut-3′ UTR. (b) Firefly luciferase reporter that contained AQP4 3′ UTR and AQP4 mut-3′ UTR. (c) Bar graph represented relative luciferase activity in AW, AW+b and AM+b. $^{**}P < 0.01$, data are mean ± s.d., three independent experiments. AW: AQP4 wild-type 3′ UTR; AW+b: AQP4 wild-type 3′ UTR+ miR-29b mimic; AM+b: AQP4 mutant 3′ UTR+ miR-29b mimic.

It is clear that miRNAs have important roles in ischemic brain injury. Application of miRNA profiling techniques (microarray analysis) in ischemic brain injury started from 2008. Changes in miRNAs including miR-29 family members (Table 1) have been identified in rodent focal ischemia model and forebrain ischemia model as well as in clinical stroke patients.[29–31] The profiling changes of miR-29 s after cerebral ischemia vary depending on the type and location of brain ischemia. The miR-29 family was downregulated in the cortex after focal ischemia,[29] while it was upregulated in the hippocampus after forebrain ischemia.[30] Using RT-qPCR techniques, it was found that miR-29a expression increased in the ischemia-resistant hippocampal dentate gyrus area and decreased in the vulnerable CA1 area in a rat forebrain ischemia model.[32] The loss of miR-29b in the infarct region contributed to the injury of focally ischemic brain.[13] Another study reported that the miR-29b increased after cerebral ischemia. However, this study measured miR-29b in whole brain after stroke, which might mask changes in different focal region. It was unclear whether the increase was primarily on the contralateral hemisphere.[33] Using the same technique, we found that miR-29b expression was significantly downregulated in the circulating blood of the patients with ischemic stroke and in both the blood and the brain of mice after MCAO. We further showed that miR-29b expression was negatively correlated with stroke outcomes, NIHSS scores, and brain infarct volume. The circulating miR-29b increased in patients with better outcomes compared with those with poor outcomes. To our knowledge, it is the first time to show that circulating miR-29b level is correlated with the recovery after cerebral ischemia. Stroke is a neurologic emergency where time has an extraordinary value for clinical or therapeutic

Table 1. miR-29 family and cerebral ischemia

miR-29	*Species*	*Type of ischemia*	*Change of miR-29*	*Detection method*	*Targets*	*Treatment*	*References*
a, b, c	Rat	Focal	Decrease in brain	Microarray	N/D	N/D	Jeyaseelan *et al*[29]
b, c	Rat	Focal	Decrease in brain	Microarray	N/D	N/D	Dharap *et al*[11]
b, c	Human	Young Stroke	Increase in blood	Microarray	N/D	N/D	Tan *et al*[31]
a, b, c	Rat	Global	Increase in Hippocampus	Microarray	N/D	N/D	Yuan *et al*[30]
b	Rat	Focal	Increase in brain	RT-qPCR	BCL2L2	N/D	Shi *et al*[33]
a	Rat	Global	Decrease in hippo. CA1, increase in hippo. DG	RT-qPCR	BBC3	Overexpress miR-29a in CA1	Ouyang *et al*[8,32]
b	Mouse	Focal	Decrease in brain	RT-qPCR	N/D	Overexpress	Khanna *et al*[13]
c	Mouse	Focal	Decrease in brain	RT-qPCR	DNMT3a	Overexpress	Pandi *et al*[43]
b	Human Mouse	Old stroke, Stroke	Decrease in blood and brain	RT-qPCR	AQP4	Overexpress	This study

AQP4, aquaporin 4; BBC3, BCL2 binding component 3; DG, dentate gyrus; DNMT3a, DNA methyltransferase 3a; miR-29a, microRNA-29a; N/D, no information about the target genes of miR29.

decisions. Developing a novel technique to quickly detect the changes of miR-29b will greatly help with the diagnosis and prognosis of stroke.

We understand that blood sample tubes with RNA stabilizing agent are better than EDTA tubes. We used EDTA tube in this research because this tube is commonly used in the clinic. Considering that RNA might degrade, we processed the blood sample immediately after sample collection. The integrity and concentration of total RNA was stably preserved in the samples. The absorbance of samples at 260/280 nm ranged between 1.8 and 2.0, suggesting that this method is feasible and acceptable.

The functional significance of unique miRNAs in ischemic brain damage was brought to attention when miR-497 and miR-181 were found to promote ischemic neuronal death by negatively regulating anti-apoptotic proteins and molecular chaperones.[34,35] However, the miR-29 family has the opposite function compared with miR-497 and miR-181. miR-29a targeted pro-apoptotic protein PUMA and reduced neuronal vulnerability to forebrain ischemia.[32] Although in neuronal maturation research miR-29b was first found as a novel inhibitor of neuronal apoptosis through targeting pro-apoptotic BH3-only genes.[12] In this work, we first identified that miR-29b possibly targeted AQP4 under focal cerebral ischemic condition in mice.

Whether circulating miR-29b could reflect the response of brain tissue to ischemia was unclear. Furthermore, changes of miRNAs in circulation resulting from secretion by injured cells were also not well characterized. The correlation between circulating miR-29b expression and brain miR-29b expression needed to be investigated. The human blood RNA in EDTA tube could be degraded rapidly. Therefore, we detected miR-29b not from serum or plasma, but from white blood cells. We found that miRNA-29b in white blood cells was relatively stable. We found that the expression of circulating miR-29b was well correlated with brain miR-29b, suggesting that circulating miR-29b could be a indicator not only for the diagnosis and prognosis but also for the treatment of ischemic stroke. It is impossible to acquire human brain sample for miR-29b analysis clinically. It is also difficult to distinguish where the blood miR-29b came from. The best way could be to examine the exosomal miR-29b, which is the place where many microRNAs located.[36] Nevertheless, our data suggested that white blood cell miR-29b correlated with the brain miR-29b. Then, we used animal model to explore the possible regulation mechanism of brain miR-29b and AQP4 in brain tissue. Delivery of miR-29b mimic reduced 50% of stroke-induced brain lesion after 48 hours transient cerebral ischemia.[13] We found that miR-29b overexpression reduced brain infarct volume, alleviated brain edema, and attenuated the BBB damage. However, Shi *et al*[33] found that upregulated miR-29b promoted neuronal cell death after ischemic brain injury.[33] This difference could be caused by differences in model systems, timing of sample analysis, and source cells or tissues chosen for analysis.

After ischemic brain injury, the BBB permeability integrity was disrupted and the changed osmotic pressure drove water into astrocytes which eventually caused astrocytes swelling, dysfunction, and death.[1] The AQP4 upregulation was closely involved in this process. Inhibiting AQP4 upregulation protected the mouse brain from edema in stroke models.[6] During brain cell specification, miR-29 was expressed more in astrocytes than in neurons.[37] Our study showed that miR-29b expression was downregulated and AQP4 expression was upregulated after cerebral ischemia; however, the relationship between them was unexplored. With the help of bioinformatic-based databases[14] and published reports, we then validated the hypothesis that AQP4 was one direct target of miR-29b. Dual-luciferase reporter system clearly showed that AQP4 indeed is the downstream target for miR-29b. It was clear that astrocyte end-foot as an important component contributed to forming the BBB.[38] Furthermore, astrocytes also showed the capability to promote tight junction formation in the brain microvessel endothelium.[39] Therefore, miR-29b overexpression protected BBB integrity maybe through inhibiting AQP4 expression to alleviate astrocyte swelling. Until now, only two miRNAs, miR-320a and miR-130a, were known to function as modulators of AQP4,[15] of which miR-130a could bind to the AQP4 M1 promoter to repress its transcription. We now identified that miR-29b, as a newly discovered regulator of AQP4, provided a unique target for stroke treatment. A single gene may be regulated by several potential miRNAs, and this was the case for AQP4.

We injected viral vector into mice at 14 days before MCAO surgery. This is unlikely to be directly applied to clinical treatments of stroke. However, the purpose of our study is to prove the principle. miRMiR-29b overexpression reduced brain infarct volume and brain edema possibly via inhibiting AQP4 expression. However, ischemic stroke was a complicated pathologic process, which could be affected by many substances, such as oxidative stress, inflammatory cytokines, and toxic glutamate. Thus, it is insufficient for the complete recovery of ischemic stroke via only upregulating miR-29b expression. We will further explore the potential regulatory mechanism of miR-29b and develop novel technique to help the diagnosis and prognosis of stroke. The researches of the function of miR-29 had revealed controversies in ischemia research as in cancer research.[40] While down-regulation of miR-29 protected hearts against ischemia-reperfusion injury[41] and rat cortical neuronal death *in vitro*,[33] upregulation of miR-29 protected neurons from apoptosis, during neuronal maturation forebrain, and focal ischemia.[12,13] As the miR-29 family can target both pro- and anti-apoptotic BcL2 family members,[42] the controversial effects of miR-29 mentioned above might reflect inhibition of different targets in different cells under different physiologic or

pathologic settings. Further investigations would help to shed more light on miR-29 s function in different pathologic backgrounds.

CONCLUSIONS

We first report in this study that miR-29b overexpression reduces brain infarct volume, alleviates brain edema, and attenuates BBB damage, possibly by targeting AQP4. The results of this study indicate that miR-29b is a potential biomarker and therapeutic agent for treatment of cerebral ischemia.

AUTHOR CONTRIBUTIONS

YW involved in experimental design, collection and/or assembly of data, data analysis and interpretation, draft and revised manuscript. JH performed MCAO animal model and assembly of data. YM contributed to data analysis and draft the figures and revised manuscript. GT and YL performed immunohistochemistry from animal experiments. XC, ZZ, and LZ contributed to correction of human blood sample and perform miRNA analysis. Y-BO and YW contributed to data analysis and interpretation and involved in manuscript writing. G-YY contributed to supervising experimental design, data analysis and interpretation, manuscript writing, and final approval of manuscript.

DISCLOSURE/CONFLICT OF INTEREST

The authors declare no conflict of interest.

REFERENCES

1 Fu X, Li Q, Feng Z, Mu D. The roles of aquaporin-4 in brain edema following neonatal hypoxia ischemia and reoxygenation in a cultured rat astrocyte model. *Glia* 2007; **55**: 935–941.
2 Vella J, Zammit C, Di Giovanni G, Muscat R, Valentino M. The central role of aquaporins in the pathophysiology of ischemic stroke. *Front Cell Neurosci* 2015; **9**: 108.
3 Rash JE, Yasumura T, Hudson CS, Agre P, Nielsen S. Direct immunogold labeling of aquaporin-4 in square arrays of astrocyte and ependymocyte plasma membranes in rat brain and spinal cord. *Proc Natl Acad Sci USA* 1998; **95**: 11981–11986.
4 Badaut J, Lasbennes F, Magistretti PJ, Regli L. Aquaporins in brain: Distribution, physiology, and pathophysiology. *J Cereb Blood Flow Metab* 2002; **22**: 367–378.
5 Taniguchi M, Yamashita T, Kumura E, Tamatani M, Kobayashi A, Yokawa T *et al.* Induction of aquaporin-4 water channel mrna after focal cerebral ischemia in rat. *Brain Res Mol Brain Res* 2000; **78**: 131–137.
6 Manley GT, Fujimura M, Ma T, Noshita N, Filiz F, Bollen AW *et al.* Aquaporin-4 deletion in mice reduces brain edema after acute water intoxication and ischemic stroke. *Nat Med* 2000; **6**: 159–163.
7 Tang G, Liu Y, Zhang Z, Lu Y, Wang Y, Huang J *et al.* Mesenchymal stem cells maintain blood-brain barrier integrity by inhibiting aquaporin-4 up-regulation after cerebral ischemia. *Stem Cells* 2014; **32**: 3150–3162.
8 Ouyang YB, Stary CM, Yang GY, Giffard R. Micrornas: Innovative targets for cerebral ischemia and stroke. *Curr Drug Targets* 2013; **14**: 90–101.
9 Bartel DP. Micrornas, Genomics, biogenesis, mechanism, and function. *Cell* 2004; **116**: 281–297.
10 Kriegel AJ, Liu Y, Fang Y, Ding X, Liang M. The mir-29 family: Genomics, cell biology, and relevance to renal and cardiovascular injury. *Physiol Genomics* 2012; **44**: 237–244.
11 Dharap A, Bowen K, Place R, Li LC, Vemuganti R. Transient focal ischemia induces extensive temporal changes in rat cerebral microrna ome. *J Cereb Blood Flow Metab* 2009; **29**: 675–687.
12 Kole AJ, Swahari V, Hammond SM, Deshmukh M. Mir-29b is activated during neuronal maturation and targets bh3-only genes to restrict apoptosis. *Genes Dev* 2011; **25**: 125–130.
13 Khanna S, Rink C, Ghoorkhanian R, Gnyawali S, Heigel M, Wijesinghe DS *et al.* Loss of mir-29b following acute ischemic stroke contributes to neural cell death and infarct size. *J Cereb Blood Flow Metab* 2013; **33**: 1197–1206.
14 Lewis BP, Burge CB, Bartel DP. Conserved seed pairing, often flanked by adenosines, indicates that thousands of human genes are microrna targets. *Cell* 2005; **120**: 15–20.
15 Sepramaniam S, Armugam A, Lim KY, Karolina DS, Swaminathan P, Tan JR *et al.* Microrna 320a functions as a novel endogenous modulator of aquaporins 1 and 4 as well as a potential therapeutic target in cerebral ischemia. *J Biol Chem* 2010; **285**: 29223–29230.
16 Sepramaniam S, Ying LK, Armugam A, Wintour EM, Jeyaseelan K. Microrna-130a represses transcriptional activity of aquaporin 4 m1 promoter. *J Biol Chem* 2012; **287**: 12006–12015.
17 Special report from the National Institute of Neurological Disorders and Stroke. Classification of cerebrovascular diseases III. *Stroke* 1990; **21**: 637–676.
18 Kasner SE. Clinical interpretation and use of stroke scales. *Lancet Neurol* 2006; **5**: 603–612.
19 Sims JR, Gharai LR, Schaefer PW, Vangel M, Rosenthal ES, Lev MH *et al.* Abc/2 for rapid clinical estimate of infarct, perfusion, and mismatch volumes. *Neurology* 2009; **72**: 2104–2110.
20 Schmittgen TD, Livak KJ. Analyzing real-time pcr data by the comparative c (t) method. *Nat Protoc* 2008; **3**: 1101–1108.
21 Boyden ES, Zhang F, Bamberg E, Nagel G, Millisecond-timescale Deisseroth K. genetically targeted optical control of neural activity. *Nat Neurosci* 2005; **8**: 1263–1268.
22 Tiscornia G, Singer O, Verma IM. Production and purification of lentiviral vectors. *Nat Protoc* 2006; **1**: 241–245.
23 He X, Li Y, Lu H, Zhang Z, Wang Y, Yang GY. Netrin-1 overexpression promotes white matter repairing and remodeling after focal cerebral ischemia in mice. *J Cereb Blood Flow Metab* 2013; **33**: 1921–1927.
24 Yang G, Chan PH, Chen J, Carlson E, Chen SF, Weinstein P *et al.* Human copper-zinc superoxide dismutase transgenic mice are highly resistant to reperfusion injury after focal cerebral ischemia. *Stroke* 1994; **25**: 165–170.
25 Huang J, Li Y, Tang Y, Tang G, Yang GY, Wang Y. Cxcr4 antagonist amd3100 protects blood-brain barrier integrity and reduces inflammatory response after focal ischemia in mice. *Stroke* 2013; **44**: 190–197.
26 Tanno H, Nockels RP, Pitts LH, Noble LJ. Breakdown of the blood-brain barrier after fluid percussive brain injury in the rat. Part 1: Distribution and time course of protein extravasation. *J Neurotrauma* 1992; **9**: 21–32.
27 Bauer AT, Burgers HF, Rabie T, Marti HH. Matrix metalloproteinase-9 mediates hypoxia-induced vascular leakage in the brain via tight junction rearrangement. *J Cereb Blood Flow Metab* 2010; **30**: 837–848.
28 Vlachos IS, Hatzigeorgiou AG. Online resources for mirna analysis. *Clin Biochem* 2013; **46**: 879–900.
29 Jeyaseelan K, Lim KY, Armugam A. Microrna expression in the blood and brain of rats subjected to transient focal ischemia by middle cerebral artery occlusion. *Stroke* 2008; **39**: 959–966.
30 Yuan F, Wang Y, Guan Y, Lu H, Xie B, Tang Y *et al.* Microangiography in living mice using synchrotron radiation. 2010; **1266**: 68.
31 Tan KS, Armugam A, Sepramaniam S, Lim KY, Setyowati KD, Wang CW *et al.* Expression profile of micrornas in young stroke patients. *PLoS One* 2009; **4**: e7689.
32 Ouyang YB, Xu L, Lu Y, Sun X, Yue S, Xiong XX *et al.* Astrocyte-enriched mir-29a targets puma and reduces neuronal vulnerability to forebrain ischemia. *Glia* 2013; **61**: 1784–1794.
33 Shi G, Liu Y, Liu T, Yan W, Liu X, Wang Y *et al.* Upregulated mir-29b promotes neuronal cell death by inhibiting bcl2l2 after ischemic brain injury. *Exp Brain Res* 2012; **216**: 225–230.
34 Yin KJ, Deng Z, Huang H, Hamblin M, Xie C, Zhang J *et al.* Mir-497 regulates neuronal death in mouse brain after transient focal cerebral ischemia. *Neurobiol Dis* 2010; **38**: 17–26.
35 Ouyang YB, Lu Y, Yue S, Giffard RG. Mir-181 targets multiple bcl-2 family members and influences apoptosis and mitochondrial function in astrocytes. *Mitochondrion* 2012; **12**: 213–219.
36 Sahoo S, Losordo DW. Exosomes and cardiac repair after myocardial infarction. *Circ Res* 2014; **114**: 333–344.
37 Mor E, Cabilly Y, Goldshmit Y, Zalts H, Modai S, Edry L *et al.* Species-specific microrna roles elucidated following astrocyte activation. *Nucleic Acids Res* 2011; **39**: 3710–3723.
38 Abbott NJ, Ronnback L, Hansson E. Astrocyte-endothelial interactions at the blood-brain barrier. *Nat Rev Neurosci* 2006; **7**: 41–53.
39 Lee SW, Kim WJ, Choi YK, Song HS, Son MJ, Gelman IH *et al.* Ssecks regulates angiogenesis and tight junction formation in blood-brain barrier. *Nat Med* 2003; **9**: 900–906.
40 Pekarsky Y, Croce CM. Is mir-29 an oncogene or tumor suppressor in cll? *Oncotarget* 2010; **1**: 224–227.
41 Ye Y, Perez-Polo JR, Qian J, Birnbaum Y. The role of microrna in modulating myocardial ischemia-reperfusion injury. *Physiol Genomics* 2011; **43**: 534–542.
42 Ouyang YB, Xu L, Yue S, Liu S, Giffard RG. Neuroprotection by astrocytes in brain ischemia: Importance of micrornas. *Neurosci Lett* 2014; **565**: 53–58.
43 Pandi G, Nakka VP, Dharap A, Roopra A, Vemuganti R. MicroRNA miR-29c down-regulation leading to de-repression of its target DNA methyltransferase 3a promotes ischemic brain damage. *PLoS One* 2013; **8**: e58039.

Supplementary Information accompanies the paper on the Journal of Cerebral Blood Flow & Metabolism website (http://www.nature.com/jcbfm)